JOURNAL OF GEOPHYSICAL RESEARCH, VOL. 106, NO. A7, PAGES 13,135–13,144, JULY 1, 2001

A case study test of Araki's physical model of geomagnetic sudden commencement

M. M. Lam and A. S. Rodger

British Antarctic Survey, Natural Environment Research Council, Cambridge, England, U.K.

Abstract. This paper tests the *Araki* [1994] computational model of the Earth–ionosphere system during geomagnetic sudden commencement (sc). In particular, we test the model's ability to predict the signs of the preliminary and main impulses, given the latitude and the magnetic local time (MLT), using a case study of an sc which occurred at 0949 UT on November 22, 1997. Data from a global network of magnetometer stations and from satellites are used. Model predictions compare well with the case study data at high latitudes (above $\sim 72°$N Altitude Adjusted Corrected Geomagnetic Coordinates (AACGM)), less well for lower latitudes, particularly on the nightside. In addition, the position of the footprints of the field–aligned currents (FACs) associated with the sc ground signature varies with MLT, contrary to the model. Data from satellites in polar and geostationary orbits suggest that the FACs for both the preliminary and the main impulses map to gradients in magnetospheric plasma concentration, such as the outer radiation belt and the plasmapause.

1. Introduction

Sudden changes in the solar wind dynamic pressure, caused by interplanetary shocks and discontinuities, can give rise to the phenomenon known as the geomagnetic sudden commencement (sc), in which a clear onset is observed almost simultaneously (usually within minutes) everywhere within the magnetosphere and on the ground. *Araki* [1994] provides the simplest description and most comprehensive explanation of the ground magnetic signature due to a geomagnetic sudden commencement. Araki also presents the results of a computational model which calculates the magnetic disturbance at the Earth's surface due to the sc current system. The aim of our work is to test Araki's computational model against a case study which makes use of magnetometer and satellite data. In Araki's conceptual model, the field–aligned currents (FACs) of the preliminary impulse map out to regions of significant gradient in plasma concentration and magnetic field; however, this is not reflected in his computational model, where the latitude of the FACs is set to a constant 75°N Corrected Geomagnetic Coordinates (CGM) in the ionosphere. We present evidence that FACs map to both the poleward boundary of the outer radiation belt and to the plasmapause. *Moretto and Yahnin* [1998] have made similar suggestions regarding the mapping of FACs associated with observations of traveling convection vortices (TCVs). Similarly, *Slinker et al.* [1999] find that the ionospheric FACs, in a global three–dimensional MHD simulation of the Earth's response to a solar wind density pulse, map to a radial distance of $\sim 7\ R_E$ in the equatorial plane, well away from the magnetopause and the low–latitude boundary layer (LLBL). The evolution of the sc and its ionospheric signature are strongly controlled by the wave propagation characteristics of the inhomogeneous magnetospheric structure in this simulation.

In section 1.1 we review the theoretical ideas and observations related to sc's presented by *Araki* [1994]. We then examine (section 1.2) the computational model of *Araki* [1994] and its predictions. In section 2 we present a case study of an sc event and compare it directly with predictions from the Araki computational model. In particular, we concentrate on the distribution of the sign of the preliminary and the main impulses with magnetic latitude and magnetic local time (MLT). We use Defense Meteorological Satellite Program (DMSP) satellite data to select the most appropriate statistical auroral oval for our case study. National Oceanic and Atmospheric Administration (NOAA) satellite data are used to locate the high–energy ion–trapping boundary at one point on the nightside and at one on the dayside. Data from the Los Alamos National Laboratory (LANL) 1994 geostationary satellite are used to find the position of the plasmapause close to dusk. The latitudes of the oval, the ion–trapping boundaries, and the plasmapause in the ionosphere are compared to the observed latitude for the footprints of the FACs associated with the case study event. In section 3 we consider the evidence provided by the case study in support of the proposition that the field-aligned currents for both the

Paper number 2000JA900134.
0148-0227/01/ 2000JA900134$09.00

preliminary and main impulses of the sc ground signature map to gradients in the magnetospheric plasma concentration. Section 4 contains our conclusions.

1.1. *Araki*'s [1994] Conceptual Model of sc's

Araki's [1994] conceptual model of sc's results from a large number of observations and theoretical ideas in the literature. *Araki* [1994] summarizes the observations on the ground of an sc onset for an increase in solar wind dynamic pressure as follows (the signature is reversed for pressure decrease): The signature of the sc in the H component of the magnetic field consists of two successive pulses with opposite senses at high latitudes, the first is known as the preliminary pulse (PI) and the second is known as the main impulse (MI). If PI is positive, it is termed a preliminary positive impulse (PPI), and if it is negative, it is termed a preliminary reverse impulse (PRI). At auroral latitudes a positive pulse precedes a negative one in the morning, and the sign of the pulses is reversed in the afternoon. For the polar cap the situation is the other way round, with the positive pulse preceding the negative in the afternoon and the negative pulse being first in the morning. At middle and low latitudes the waveform of the H component becomes increasingly like a ramp, still retaining the two–pulse structure with the amplitude of the pulses decreasing with decreasing latitude. At the equator the two–pulse structure is present on the dayside but absent on the nightside, which experiences at most a PPI.

Araki's [1994] proposal is that the variety of forms for the sc signature, as measured by the magnetic field on the surface of the Earth, derives from three signals which each vary with MLT and latitude in a fairly simple way. Araki divides the sc signature close to the Earth's surface into two parts:

$$D_{sc} = DL + DP. \tag{1}$$

In the case of a stepwise increase in the solar wind dynamic pressure, DL is a "dc–like" step up in the magnetic field, and DP is a two–pulse signal. The two–pulse signal is itself proposed to be made up of the sharp preliminary impulse and the following main impulse:

$$DP = DP_{pi} + DP_{mi}. \tag{2}$$

When the magnetosphere is compressed by a shock wave in the solar wind, the dawn–to–dusk magnetopause electric current increases to a value J_M. The current produces an increase of the magnetic field in the magnetosphere, and the magnetospheric plasma responds by producing a dusk–to–dawn polarization current J_p. The force J_pxB produces a compression of the magnetospheric plasma which propagates earthward as a fast–mode compressional hydromagnetic wave. The northward magnetic field is increased inside the current loop formed by the magnetopause and polarization currents. When the wave front reaches the ionosphere, the polarization current J_p is converted to a westward conduction current, the Earth current is induced in the same direction, and the magnetic H component begins to increase on the ground. This increase, referred to by *Araki* [1994] as DL, is caused by the entire current system flowing on the magnetopause and in the magnetosphere, the ionosphere, and the Earth.

At points where there is a sufficient gradient in the magnetospheric plasma concentration and the magnetic field, the fast–mode compressional wave is converted into an Alfvén wave which, accompanied by an FAC, flows along field lines into the ionosphere on the duskside and out of the ionosphere on the dawnside. The circuit is completed in the ionosphere by twin–vortex currents, which, in the Northern Hemisphere, flow in a clockwise direction in the afternoon and in an anticlockwise direction in the morning. Since this current system has been deduced from measurement of the magnetic disturbance produced on the ground, both the ground magnetic response and the equivalent current system are labeled as DP_{pi}, even though the magnetic response on the ground is produced by more than just the currents flowing in the ionosphere.

The main impulse, DP_{mi}, is a result of the adjustment of the magnetosphere to its new compressed state. A transient convection electric field is produced in the dusk–to–dawn direction, which is associated with a pair of FACs flowing into the dawn ionosphere and out of the dusk ionosphere (in the opposite sense to the DP_{pi}). A twin–vortex current system of the DP 2 type, which has the opposite sense to the preceding DP_{pi} current system, is produced in the ionosphere and is a large contributor to the main impulse field, DP_{mi}, on the ground. The signal for both the preliminary and main impulses in the polar ionosphere propagates as an electromagnetic wave to the equator via the Earth-ionosphere waveguide.

1.2. The Computational Model of *Araki* [1994]

Araki [1994] designed a simple computational model from the conceptual ideas presented in section 1.1. In the computational model, a pair of FACs, C1, associated with the DP_{pi} field, flow into (out of) the afternoon (morning) polar ionosphere symmetrically about the noon meridian. The footprints of C1 move along the 75°N CGM latitudinal circle from noon to the eveningside and morningside, their intensities varying from zero to a maximum and then back to zero over a period of 9 min. The movement of the footprints of the FACs C1 is designed to produce the effect of the solar wind discontinuity moving down the flanks of the magnetopause: The continuous generation of fast–mode waves which intersect a gradient in plasma concentration and magnetic field first close to noon and then at MLTs ever closer to dusk and dawn, causes Alfvén wave and FAC production to also move from noon to dawn and dusk. A second pair of FACs, C2, responsible for DP_{mi}, begins to flow into (out of) the morning (afternoon) polar ionosphere 4.5 min after the first set of FACs do so. The

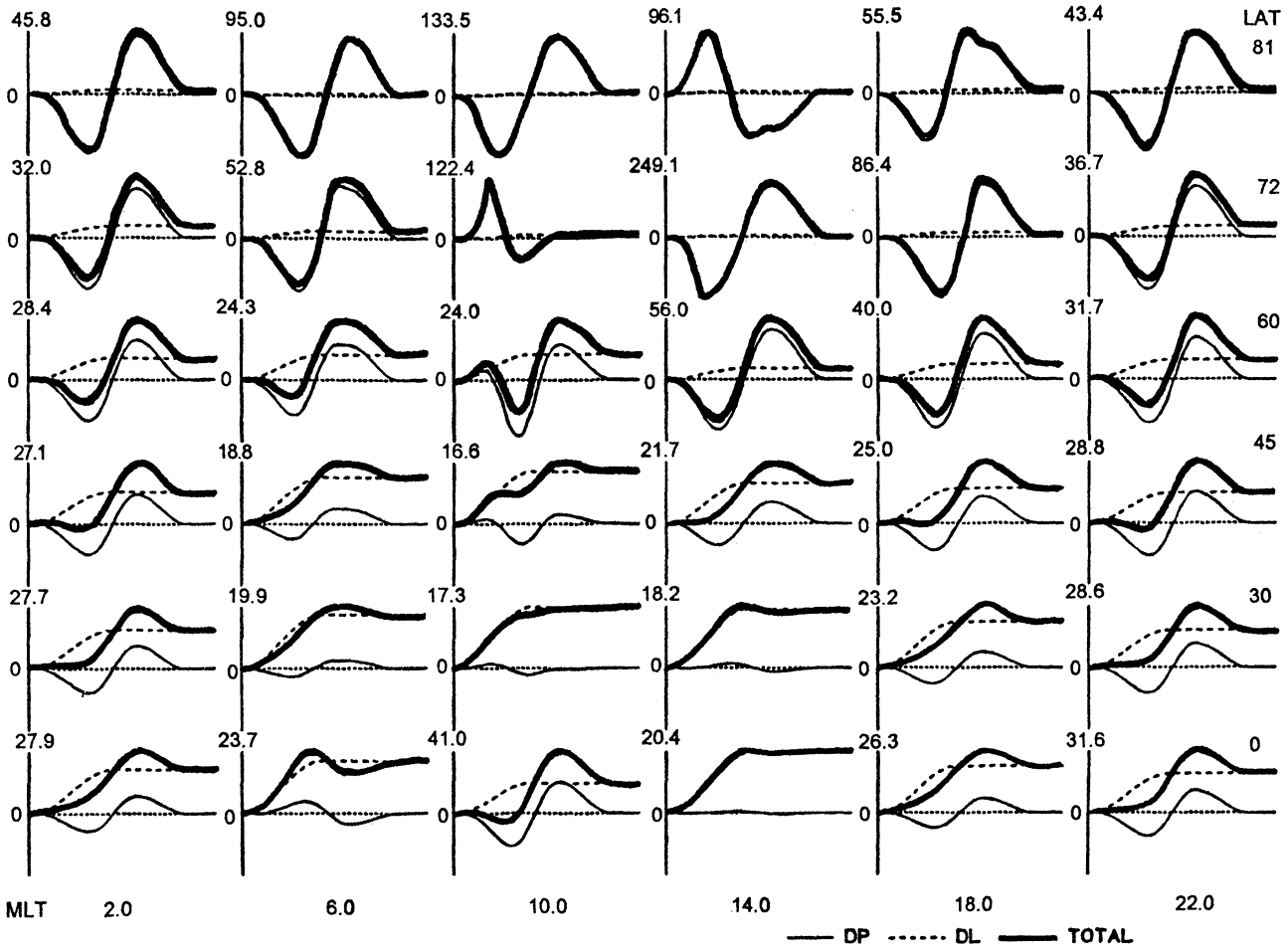

Figure 1. A reproduction of Figure 5 of *Osada* [1992], which shows profiles of the H component of the ground magnetic field for the *Araki* [1994] computational model. The number at the top left of each graph indicates the scale value of the graph (nT). The lighter solid lines and the dashed lines represent DP and DL, respectively, the bold lines show the total field, and the dotted lines show H=0.

footprints of the currents C2 are fixed at 0840 and 1520 MLT and at 75°N CGM, and their intensities vary in a similar manner to those of C1. The values for the parameters are chosen by Araki so that the model displays the general characteristics of the worldwide distribution of sc fields.

The method of calculation is as follows: The global distribution of ionospheric currents associated with DP_{pi} and DP_{mi} is found using the continuity equation on a thin shell ionosphere with realistic conductivities. The ground magnetic fields produced by the ionospheric currents and FACs are calculated using the Biot–Savart law. A time–dependent value for the H component of DL is added to the H component of the magnetic disturbance, DP. Note that the latitude of the footprints of the FACs for DP_{pi} in the computational model is a constant, which is unlikely to reflect Araki's proposal that the FACs map out to a plasma concentration gradient in the magnetosphere.

Detailed results of this model are available from the thesis of Araki's student, [*Osada*, 1992], there being just a summary of the model and its results in *Araki*'s [1994] paper. The H component of the ground magnetic field is presented in Figure 5 of *Osada*'s [1992] thesis, reproduced here as Figure 1. It gives the total signal, D_{sc}, the ramp DL, and the transient signal, DP, for a selection of latitudes and MLTs. In Osada's study a limited investigation into the dependence of the model results on the latitude of the FACs demonstrates that the latter determines the latitude at which reversal takes place between the sc signal displaying a PPI and a PRI. For the dayside in Araki's computational model the H component magnetic field changes sign at a latitude of 75°N CGM, which is the source current region. We shall concentrate on whether the distribution of the sign of DP_{pi} in the model matches that for our case study data.

Figure 2a shows the sign of the H component of DP_{pi}, as a function of geomagnetic latitude and MLT, as given by Figure 1, for midlatitudes to high latitudes. The H component of DP_{pi} is positive for auroral latitudes in the morning, and for the polar cap in the afternoon and elsewhere it is negative. We know where the lati-

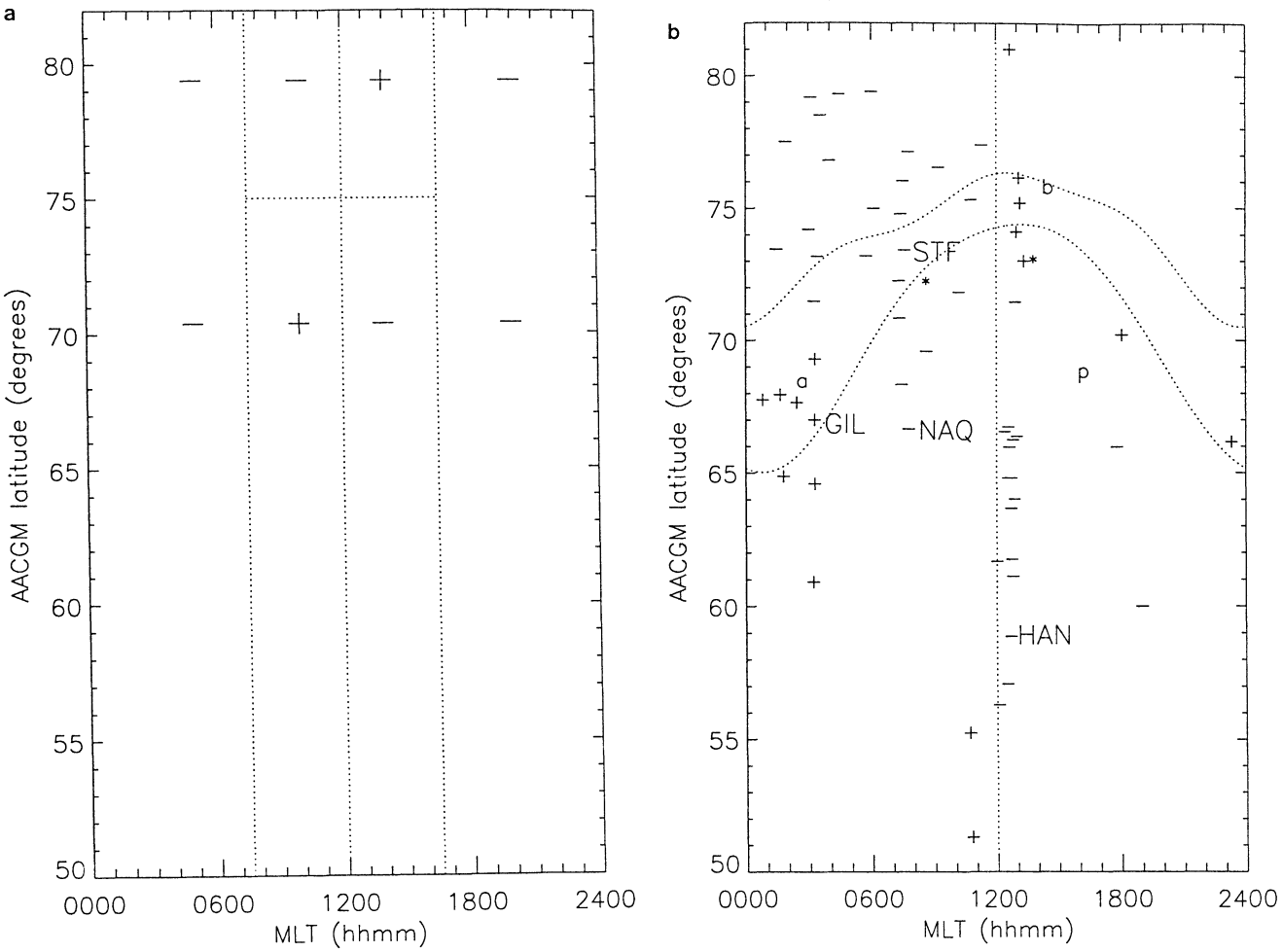

Figure 2. A map of geomagnetic latitude versus MLT showing the sign of the H component of DP_{pi} according to (a) *Araki*'s [1994] model and (b) the case study magnetometer data. The poleward and equatorward edges of the statistical auroral oval are marked by the upper and lower dotted curves. They are selected using the central plasma sheet/boundary plasma sheet (CPS/BPS) boundaries just before the event (marked by an asterisk). The ion–trapping boundary for the energy range 30–80 keV just before the event is marked "b", and that for just after is marked "a". A position for the plasmapause is marked by "p". The positions of magnetometer stations Hankasalmi (HAN), Narssarssuaq (NAQ), Gillam (GIL), and S. Stromfjord (STF) are marked and labeled.

tudinal boundary marking the change in sign of DP_{pi} occurs (75°N CGM) and that there is a similar boundary in MLT at noon, but although it is clear in Figure 1 that an additional two boundaries in MLT exist, we can only tell that they lie somewhere between 0600 and 1000 MLT, and between 1400 and 1800 MLT, respectively. The boundaries are given by the loci of the points of zero magnitude in the eastward component of the equivalent current field for the model, DP_{pi}, but this is not available in *Araki*'s [1994] paper or *Osada*'s [1992] thesis; however, a similar model due to *Tsunomura and Araki* [1984], with realistic conductivity and idealized FACs moving along a line of constant latitude, exhibits boundaries between PPIs and PRIs that lie roughly along constant MLTs, ~ 5 hours toward the nightside from the point of maximum FAC intensity. The main difference between the model of Araki and that of Tsunomura and Araki is that in the latter, the FACs span the whole of magnetic local time and are at a maximum at 0600 and 1800 MLT, while in the former they merely span the dayside and are a maximum at 0900 and 1500 MLT. Given that the boundaries in Araki's model are therefore probably displaced at least an hour or two toward the nightside from the MLT of maximum intensity, they are identified as lying at 0730 and 1630 MLT ± 90 min.

2. A Case Study

In this section, data are presented for a case study of an sc event which occurred at ~ 0949 UT on November 22, 1997. For all data, altitude–adjusted corrected

Table 1. Signature of Solar Wind Discontinuity in the Magnetic Field for Satellite Data[a]

Satellite	Position,	Magnetic Field, nT		UT	
Name	R_E	Before	After		Region
ACE	209,-50,8	-2,5,2	-5,14,6	0906	SW
Wind	181,-5,32	-2,5,-3	-8,2,-15	0914	SW
GOES 8	-1,-6,-2	-20,63,70 (96)	-24,43,70 (86)	0949	MS
GOES 9	-6,-2,-2	-1,11,50 (51)	-17,4,37 (41)	0949	MS
Interball Tail	-10,-6,-10	-36,-6,-11 (38)	-66,-13,-20 (70)	0950	MS
Geotail	-21,-15,3	11,5,9 (15)	16,13,18 (27)	0953	MS

[a]SW, solar wind; MS, magnetosphere; ACE, Advanced Composition Explorer. GOES 8 and 9 are at 0507 and 0050 MLT, respectively.

geomagnetic (AACGM) coordinates and MLTs are calculated from geographic latitude, geographic longitude, and altitude using an algorithm based on both the Definitive Geomagnetic Reference Field (DGRF) and the International Geomagnetic Reference Field (IGRF) models, available from the National Space Science Data Center (NSSDC) at http://nssdc.gsfc.nasa.gov/space. Satellite data from the magnetosphere verify that a step increase in the dynamic pressure launches a wave traveling at a velocity consistent with that of the fast mode. Data from satellites in polar and geostationary orbits are used to test whether the latitude of the FACs for the preliminary impulse maps to regions of plasma concentration gradients in the magnetosphere, where the fast–mode wave may convert to the Alfvén mode. Data from 60 magnetometer stations are used to form a map of the sign distribution of DP_{pi}, which is compared to that for *Araki*'s [1994] model.

2.1. Satellite Data

On November 22, 1997, the satellite Wind (see Table 1) for the location) recorded a fourfold step–like increase in the solar wind dynamic pressure, $P = m_i n_i |V_x|^2$, which, according to the 3–s resolution data, occurred during an interval of $\sim$ 9 s. The increase in pressure can be seen close to 0913 UT in Figure 3, marked by the vertical dotted line labeled "(i)". From the top the fields in Figure 3 are the following: the x component of the solar wind ion velocity, V_x; the ion number density, n_i; and the three components of the interplanetary magnetic field (IMF), B_x, B_y, and B_z. The coordinate system for the magnetic field in Figure 3 is GSM. For the 30 min preceding the step increase in pressure, the IMF is constant at $\sim$ (-1,5,0) nT. Between 0914 and 0922 UT each component of the IMF varies by at least 6 nT. This is the signature of the discontinuity in the solar wind which causes an sc at the Earth. The vertical dotted lines labeled "(ii)" and "(iii)" mark a minimum in IMF B_z and a northward turning in IMF B_z, respectively. Table 1 gives the positions of six satellites and the magnetic field which their

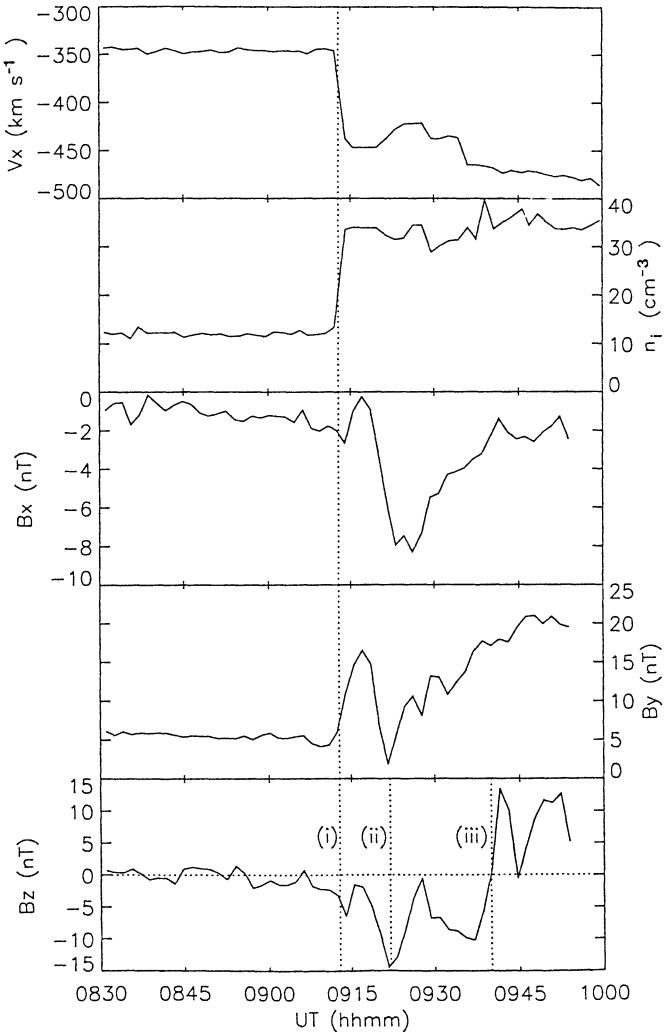

Figure 3. Solar wind data as provided by the Wind satellite. From the top the panels are the following: the x component of the solar wind ion velocity, V_x; ion number density, n_i; and the three components of the interplanetary magnetic field (IMF), B_x, B_y, and B_z. The coordinate system is GSM. The vertical dotted lines mark the times at which there are a step in the solar wind dynamic pressure, "(i)", a minimum in the IMF B_z, "(ii)", and a change from southward to northward IMF B_z, "(iii)".

Table 2. Particle Boundaries From Satellite Data[a]

Satellite Name	UT	Geographic Coordinates, deg		AACGM Latitude	MLT	Symbol in Figure 2b
		Latitude	Longitude			
F-12	0940	77	36	73	1343	*
F-13	0946	67	322	72	0835	*
N-12	0940	81	61	76	1508	b
N-14	1001	-73	215	69	0301	a
L-94	0949	0	103	69	1631	p

[a]AACGM, Altitude-Adjusted Corrected Geomagnetic Coordinates; F-12 and F-13 are Defense Meteorological Satellite Program (DMSP) satellites; N, NOAA; L-94, LANL 1994.

instruments measure directly before and after the passage of the discontinuity. The numbers in brackets are the magnitudes of the magnetic field. The changes in magnetic field are observed over a period of 10 min or less. The coordinate system in Table 1 is GSM, with the position in units of R_E. The last column gives the region of geospace occupied by the satellite.

At the Advanced Composition Explorer (ACE) satellite and at Wind there is at least a doubling in the magnitude of the magnetic field which mostly results from an increase in B_y. The remaining satellites are in the magnetosphere, mostly on the nightside. They see a response in the magnetic field between 0949 and 0952 UT, within minutes of the onset time on the ground. The changes in the magnetic field data in the magnetosphere take 2–3 min. The event propagates from the Geostationary Operational Environmental Satellite (GOES) 8 to Geotail in $\sim$ 3 min, which is consistent with the signal being propagated at the magnetospheric fast-mode velocity ($\sim$ 1000 km s^{-1}). The magnetic fields at Interball Tail and Geotail, at 10 and 21 R_E tailward of the Earth, simply double in magnitude but do not change direction significantly. GOES 8 and 9, both 6.6 R_E from the Earth, observe a slight decrease in magnitude of the magnetic field due to the compression and intensification of the ring current. The tail of the magnetosphere is dramatically changed by the discontinuity in the solar wind while the inner magnetosphere is relatively unaffected.

The NOAA 12 and 14 and DMSP polar-orbiting satellites and the LANL 1994 geostationary satellite are used in this study to identify particle boundaries, as has been done by *Moretto and Yahnin* [1998]. The position of the equatorward boundary of the statistical auroral oval lies close to the central plasma sheet/boundary plasma sheet (CPS/BPS) precipitation boundary. This boundary is identified in DMSP satellite data systematically using the *Newell et al.* [1991] boundary identification scheme. The CPS/BPS boundaries at 0940 and 0946 UT, just before the sc, are presented in Table 2 (satellites F-12 and F-13, respectively) and are marked in Figure 2b using an asterisk. The poleward and equatorward edges of statistical auroral ovals for an activity level of Q=2 [*Holzworth and Meng*, 1975] are superposed on Figure 2b. The AACGM coordinates and MLTs of the boundaries are accurate to within $\sim$ $\pm$ 1° and $\pm$ 30 min, respectively.

The count rate as a function of AACGM latitude, for ions within the energy range 80–250 keV and 30–80 keV, measured using the medium-energy proton and electron detector (MEPED) aboard the NOAA 12 polar-orbiting satellite, is shown in Figures 4a and 4b. Figure 4c shows the peak particle energy for ions with energy less that 20 keV as measured by the total energy detector (TED). The boundaries for the count rate are defined as an order of magnitude drop in intensity from the equatorward to the poleward side. The boundary signature in the peak energy is, moving poleward, a sharp drop in value, accompanied by an increase in the noisiness of the signal. The ion-trapping boundaries, as determined by visual inspection using these definitions, are marked in Figure 4 by vertical dotted lines. For ions in the energy range 80–250 keV (Figure 4a), there is a local maximum in the count rate at $\sim$ 69°N. Between 69° and 71°N there is a rapid fall in the count rate with latitude. There is not quite a full order of magnitude drop in intensity; nevertheless, we can locate the ion-trapping boundary at $\sim$ 70.5°N, where there is a change in the gradient and noisiness of the signal. In Figure 4b there is a magnitude fall between a local maximum and minimum in the count rate between 74° and 76°N, therefore 76°N is taken to be the ion-trapping boundary for the energy range 30–80 keV. It is easy to spot the boundary signature in the peak energy at $\sim$ 77°N (Figure 4c). From the scale on the x axis one can deduce that the accuracy of the AACGM latitude is to within $\sim$ $\pm$ 1°. The MLTs of the boundaries are accurate to within $\sim$ $\pm$ 30 min. Table 2 contains the positions of ion-trapping boundaries in the energy range 30–80 keV before and after the sc, as derived from NOAA 12 and 14 satellite data, respectively. A value for the ion-trapping boundary in the Northern Hemisphere for NOAA 14 has been calculated from the value in the Southern Hemisphere assuming geomagnetic conjugacy. The ion-trapping boundaries before and after the sc, for the energy range 30–80 keV, are plotted in

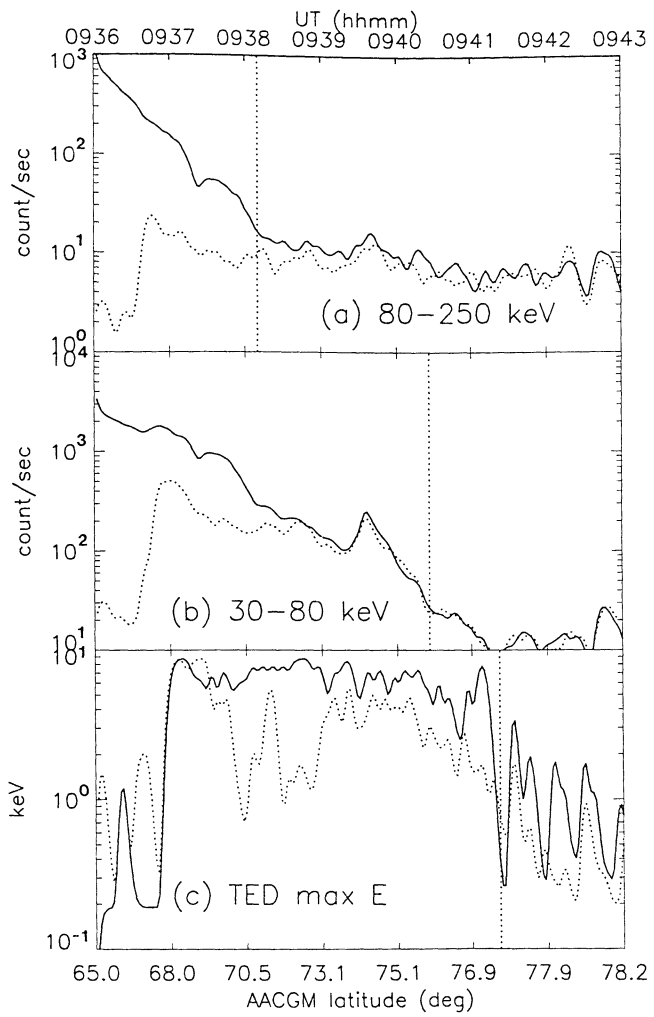

Figure 4. NOAA 12 high–energy ion data. The dotted lines show the flux along the magnetic field lines (precipitating), and the solid lines show the flux close to perpendicular to the field lines (trapped). The count rate is shown for ions within the energy range (a) 80–250 keV and (b) 30–80 keV. (c) The peak particle energy for ions with energy less that 20 keV. The ion–trapping boundaries, as determined by visual inspection, are marked in Figure 4 by vertical dotted lines.

Figure 2b at 0940 UT (marked "b" which stands for "before") and at 1001 UT (marked "a" which stands for "after").

The partial concentration of low–energy ions (1-130 eV e^{-1}), as obtained from the Magnetospheric Plasma Analyser (MPA) aboard the LANL 1994 satellite, drops from $\sim$ 80 cm^{-3} to $\sim$ 5 cm^{-3} at 0949 UT (not shown). For several hours preceding the sc, LANL 1994 passes through the plasmasphere close to the outer edge. The compression of the magnetosphere due to the sc at 0949 UT leaves the satellite outside the plasmapause. Table 2 gives the latitude in AACGM and the MLT (accurate to well within $\pm$ 1° and $\pm$ 30 min, respectively) of the plasmapause as identified from the MPA data, and this information is marked in Figure 2b by the letter "p", which stands for "plasmapause".

2.2. Magnetometer Station Data

We examined the response from 60 magnetometer stations worldwide, from the International Monitor for Auroral Geomagnetic Effects (IMAGE), the Canadian Auroral Network for the OPEN Program Unified Study (CANOPUS), the Magnetometer Array for Cusp and Cleft Studies (MACCS), the UK Sub–Auroral Magnetometer Network (SAMNET), the 210° Magnetic Meridian (210° MM), and the Greenland (western and eastern) magnetometer arrays. The stations are in the latitude range 50°–82°N AACGM and cover a wide range of MLTs, as shown in Figure 2b, where they are identified by plus and minus signs (whose significance is discussed later). The magnetometer data sets vary in their temporal resolution from 5 s to 1 min. Either the daily mean or the quiet level has been subtracted from the data. Unfiltered data are presented, but filtered data have been examined to help determine the signs of DP_{pi} and DP_{mi}. Data are usually available either in geographic (X, Y, and Z) or geomagnetic (H, D, and Z) coordinates. To be consistent with *Araki* [1994] we examine the H component of the magnetometer data; X component data have been converted into H component using the declination values given by the data providers.

Examples of the ground magnetometer response, in the H component of the magnetic field, to the sc at 0949 UT on November 22, 1997, are shown in Figure 5, using the stations Hankasalmi (HAN), Narssarssuaq (NAQ), Gillam (GIL), and S. Stromfjord (STF), respectively. The positions of these stations are marked using their code letters on Figure 2b. These stations have been chosen in order to illustrate the appearance of the sc when it is and is not obscured by other signals. The vertical line "(i)" marks the onset of the sc, some 36 min after Wind measures the step in the solar wind dynamic pressure. The other vertical lines in Figure 5 mark when 36 min has elapsed after the minimum in IMF B_z, "(ii)", and the northward turning in IMF B_z, "(iii)", are detected at the Wind satellite (lines "(ii)" and "(iii)", respectively, in Figure 3). The magnitude of DL is too small, relative to DP, at any of the magnetometer stations to be measured. At Hankasalmi (Figure 5a), a PRI is detected at 0949 UT, immediately followed at 0952 UT by a positive MI. The latter is partially masked by a marked increase in the eastward convection which occurs between 0956 and 1000 UT owing to the decrease in IMF B_z. The convection falls off between 1010 and 1040 UT, in response to the increase in IMF B_z. At Narssarssuaq (Figure 5b), intense wave activity commences at the time of the sc, which mainly consists of a decaying sine wave of period 40 min superposed on an oscillation with a period of $\sim$ 2–3 min. This makes it difficult to measure DP_{pi} and DP_{mi}. By examining the response of stations close to NAQ and by using a 2–3 min band–pass filter in addition to a 15–min high–pass filter, it is possible to determine that the sign of DP_{mi} is positive and that DP_{pi} is likely to be negative (there is,

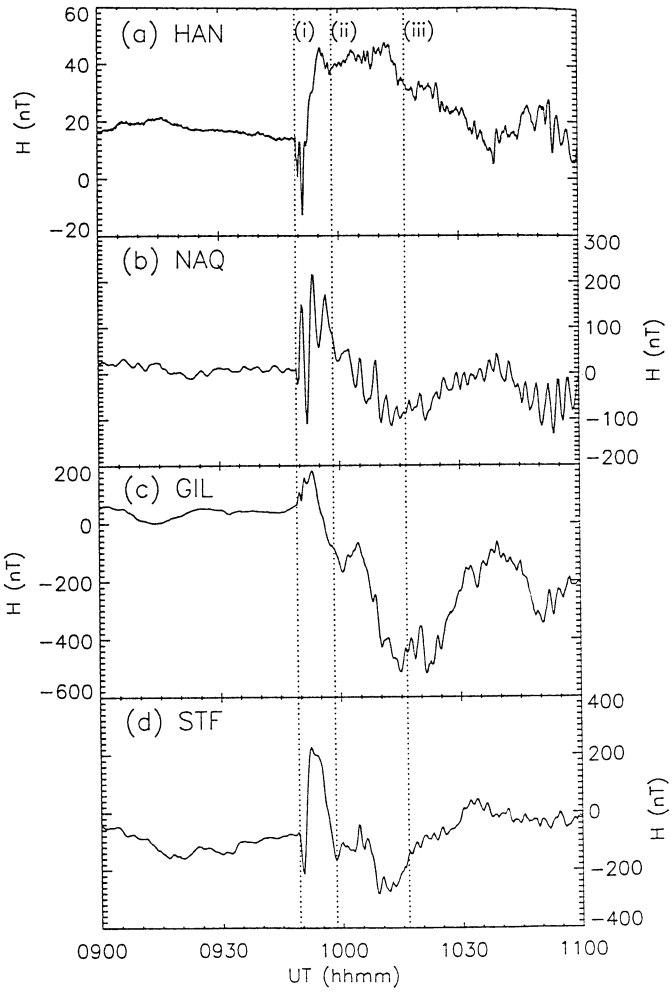

Figure 5. Examples of the H component of the ground magnetometer response at 0949 UT on November 22, 1997. The magnetometer stations concerned are (a) HAN, (b) NAQ, (c) GIL, and (d) STF. Their positions are marked in Figure 2b. At HAN and GIL the main impulse merges into the signal of the increased convection due to the decrease in IMF B_z. At NAQ, wave activity accompanies the sc onset, and at STF, DP_{pi} and DP_{mi} are easily distinguished from the background signal.

however, some uncertainty for this station). Two stations directly to the north of NAQ also measure similar wave activity after the sc, but the signs of DP_{pi} and DP_{mi} are both clearly revealed, by a 15–min high–pass filter, to be negative and positive, respectively. A PPI, followed by a negative MI, occurs at Gillam (Figure 5c), which merges into a strong negative signal in H, which is the response to the increase in westward convection. Figure 5d, at station S. Stromfjord, clearly shows the transient oscillation DP, consisting of a PRI followed by a positive MI.

The sign for DP_{pi}, for each magnetometer station in the case study data, as a function of geomagnetic latitude and local time is shown in Figure 2b. For all but five of the magnetometer stations (all clustered close to GIL), the sign of the PI is opposite to that of the MI, so that it would appear that the FACs associated with the main impulse for our case study event map out to the same region of the magnetosphere as those for the DP_{pi}. We only have significant amounts of data on the nightside in the region from 2300–0600 MLT. B_z is relatively constant before the step up in solar wind dynamic pressure, P. Since DP_{pi} lasts, on average, a maximum of 2–3 min, the relatively moderate variation in B_z which occurs during the 5 min after the step increase in P is unlikely to affect the distribution of DP_{pi} with latitude and MLT strongly.

Table 3 compares the results of *Araki*'s [1994] model (Figure 2a) with the observations of the case study here (Figure 2b). Early morning, late morning, early afternoon, and late afternoon are taken to be roughly from 0000–0600, 0600–1200, 1200–1800, and 1800–2400 MLT, respectively. One major difference between the model and the observations is in the value of the separatrix between high and lower latitudes. In the model it is at 75°N CGM in the late morning and early afternoon, but the data indicate that it lies between ~ 55°–66°N and 72°N AACGM. Table 3 demonstrates that at high latitudes (above ~ 72°N AACGM) there is good agreement at all MLTs except late afternoon, when there are no observational data. However, at lower latitudes the model does not appear to perform so successfully. The most obvious discrepancy is in the early morning, and the only certain agreement is in the early afternoon. At other times the data coverage is sparse, and any conclusion must be treated with care. Section 3 provides a few comments on these comparisons.

3. Discussion

In *Araki*'s [1994] model, the latitude of the FACs is taken to be a constant and somewhat arbitrary 75°N CGM, which may be thought to be the typical location of the open/closed field line boundary. However, the observations show good correspondence between the latitude of the ion–trapping boundary for 30–80 keV ("b" in Figure 2b) and the latitude at which the change in sign occurs for DP_{pi} and DP_{mi} at 1400 MLT. The ion–trapping boundary can provide a good location for mode conversion of a fast mode into an Alfvén mode wave which would be subsequently field–aligned guided into the ionosphere. Therefore it is suggested that the location of the FACs in the afternoon is associated with mode conversion at the ion–trapping boundary, consistent with the suggestion of *Moretto and Yahnin* [1998]. Although there are no data for this case study, the ion–trapping boundary in the morning sector may be less distinct as ions drift westward and may be lost through the dayside magnetopause into the magnetosheath. Therefore the absence of the reversal at similar latitude can be explained.

A sign reversal is observed at lower latitudes in the morning sector (between 55° and 66°N AACGM). This could be associated with the second region where fast–

Table 3. Comparison of the Sign of DP_{pi} Between *Araki*'s [1994] Model and the Case Study for High Latitudes, Above 72°N AACGM, and for Lower Latitudes[a]

	Early Morning	Late Morning	Early Afternoon	Late Afternoon
High Latitude	Y	Y	Y	...
Lower Latitude	N	N/?	Y	N/?

[a]For *Araki*'s [1994] model, see Figure 2a. For the case study see Figure 2b. Y, agreement; N, disagreement; ?, uncertain.

mode wave conversion is likely, namely, the plasmapause, being another region where there is a steep refractive index gradient. Our single measurement of the plasmapause (labeled "p" in Figure 2b) shows that there may also be good correspondence between the latitude of the plasmapause at the time of the sc and the latitude at which the change in the sign of DP_{pi} occurs at ~ 1630 MLT. There is a bulge in the plasmapause near the equatorial plane at around dusk, which means that here the plasmasphere may partially coincide with the radiation belt and that the plasmapause will lie well below 69°N for prenoon MLTs. So, the change of sign for DP_{pi} and DP_{mi} between 0700 and 1200 MLT, which occurs somewhere between 55° and 66°N AACGM, could map out to the plasmapause.

The latitude of the change of sign of DP_{pi} and DP_{mi} is just equatorward of the ion–trapping boundary just before the event, for the energy range 30–80 keV ("b" in Figure 2b). The ion–trapping boundary after the sc event ("a" in Figure 2b) is just below the latitude of the sign change for DP_{pi}. This is consistent with the increase in convection due to the drop in IMF B_z just after the sc event. So at ~ 0300 MLT, FACs may map out to the outer radiation belt. Overall, the data suggest that the FACs for both the preliminary and the main impulse are related to several different gradients in plasma concentration such as the plasmapause and the poleward boundary of the outer radiation belt. As regards the latter, FACs may map out to a region within the ion–trapping boundary (30–80 keV) and close to the CPS/BPS precipitation boundary.

The large difference between the model and the observations in the late evening and early morning is difficult to explain. Given that the B_z component of the IMF becomes more negative, one might expect the magnitude of the DP 2 current system to increase. Indeed, there is increasing evidence that there is an almost instantaneous response on the nightside ionosphere to changes in the IMF [see *Ridley et al.*, 1998; *Lockwood and Cowley*, 1999 and references therein]. However, the positive displacement between 2300 and 0300 MLT is not in the correct sense for an increase of the DP 2 current system. Although the explanation for the positive displacement remains elusive, it is interesting to note that the boundary between positive and negative disturbances lies at ~ 70°N AACGM, which is close to the poleward edge of the auroral oval. This would be where a further ion–trapping boundary occurs, and thus there is again a good probability for fast–mode wave conversion.

In this section, limited evidence has been discussed to suggest that all the sign reversals of the DP_{pi} and DP_{mi} occur at latitudes where there is likely to be steep gradients of the refractive index of the fast–mode wave. These boundaries are the ion–trapping boundary near noon, the dayside plasmapause, and the nightside ion–trapping boundary. The data examined in this study do not extend to low enough magnetic latitudes to test whether the plasmapause on the nightside is another region where mode conversion is to be observed.

4. Conclusions

The case study event fits the criteria for the sc model specified by *Araki* [1994]: The source of the sc is a simple step–like increase in the solar wind dynamic pressure, and the resulting compression of the magnetic field propagates earthward at roughly the fast–mode wave velocity. The sc ground magnetic signature was detected globally and, to within a few minutes, simultaneously at ~ 0949 UT. *Araki*'s [1994] model does not include some of the phenomena that are observed in our data set, such as the wave activity observed at NAQ.

The observed sign for DP_{pi} and DP_{mi} as a function of geomagnetic latitude and MLT corresponds well to that predicted by the computational model at high latitudes but not so well for lower latitudes, especially on the nightside. We conclude that if the FACs for the preliminary and main impulses were not confined to the dayside in the model but were extended into the nightside, then the model results would be closer to those for this particular case study. Of course, in practice the FACs may not resemble the idealized line currents in the model, and the conductivity is different for every event. The case study data are consistent with Araki's conceptual picture of fast–mode waves being converted to Alfvén waves at plasma concentration gradients in the magnetosphere. Until the physical explanation of the differences between the model and observations is clear, we do not wish to propose modifications to Araki's model.

Acknowledgments. We would like to thank the Coordinated Data Analysis Web (CDAWeb) for access to ACE, Wind, Interball, GOES, LANL, and Geotail satellite data and to the following for providing satellite magnetometer data: N. Nees at Bartol Research Institute (ACE), S. Kokubun at STELAB, Nagoya (Geotail), H. Singer at NOAA SEC (GOES), S. Romnanov at Space Research Institute, Russian Academy of Science (Interball Tail), R. Lepping at NASA GSFC (Wind). We thank K. Ogilvie at NASA GSFC for Wind plasma data, D. McCormas at LANL for LANL 1994 MPA data, I. R. Mann and D. K. Milling for the SAMNET data (SAMNET is a PPARC national facility deployed and operated by the University of York), D. Murr for the MACCs data (MACCS array is run by Boston University and Augsburg College and supported by the National Science Foundation's Magnetospheric Physics Program), J. Watermann at the Danish Meteorological Institute for the Greenland Magnetometer data, K. Shiokawa at STELAB, Nagoya, for the 210 MM magnetometer data, P. Newell for the classified DMSP satellite data, NOAA, and A. Kadokura at NIPR for the NOAA 12 and 14 satellite data, and S. Osada for permission to publish Figure 5 from his thesis. The CANOPUS instrument array was constructed and is maintained and operated by the Canadian Space Agency for the Canadian scientific community. We thank the institutes who maintain the IMAGE magnetometer array and the PI institute for IMAGE, the Finnish Meteorological Institute.

Michel Blanc thanks Hermann Opgenoorth and Tohru Araki for their assistance in evaluating this paper.

References

Araki, T., A physical model of the geomagnetic sudden commencement, in *Solar Wind Sources of Magnetospheric Ultra-Low-Frequency Waves, Geophys. Monogr. Ser.*, vol. 81, edited by M. J. Engebretson, K. Takahashi, and M. Scholer, pp. 183–200, AGU, Washington, D. C., 1994.

Holzworth, R. H., and C.-I. Meng, Mathematical representation of the auroral oval, *Geophys. Res. Lett., 2*, 377–380, 1975.

Lockwood, M., and S. W. H. Cowley, Comment on "A statistical study of the ionospheric convection response to changing interplanetary magnetic field conditions using the assimilative mapping of ionospheric elecrodynamics technique" by A. J. Ridley et al., *J. Geophys. Res., 104*, 4387–4391, 1999.

Moretto, T., and A. Yahnin, Mapping travelling convection vortex events with respect to energetic particle boundaries, *Ann. Geophys., 16*, 891–899, 1998.

Newell, P. T., S. Wing, C.-I. Meng, and V. Sigillito, The auroral oval position, structure, and intensity of precipitation from 1984 onward: An automated on-line data base, *J. Geophys. Res., 96*, 5877–5882, 1991.

Osada, S., Numerical calculation of the geomagnetic sudden commencement, M. S. thesis, Fac. of Sci., Kyoto Univ., Kyoto, March 1992.

Ridley, A. J., G. Lu, C. R. Clauer, and V. O. Papitashvili, A statistical study of the ionospheric convection response to changing interplanetary magnetic field conditions using the assimilative mapping of ionospheric electrodynamics technique, *J. Geophys. Res., 103*, 4023–4039, 1998.

Slinker, S. P., J. A. Fedder, W. J. Hughes, and J. G. Lyon, Response of the ionosphere to a density pulse in the solar wind: Simulation of traveling convection vortices, *Geophys. Res. Lett., 26*, 3549–3552, 1999.

Tsunomura, S., and T. Araki, Numerical analysis of equatorial enhancement of geomagnetic sudden commencement, *Planet. Space Sci., 32*, 599–604, 1984.

M. M. Lam and A. S. Rodger, British Antarctic Survey, Natural Environment Research Council, High Cross, Madingley Road, Cambridge CB3 0ET, England, U.K. (M.Lam@bas.ac.uk; A.S.Rodger@bas.ac.uk)

(Received April 10, 2000; revised September 12, 2000; accepted September 12, 2000.)